ФИЗИКА ЭЛЕМЕНТАРНЫХ ЧАСТИЦ И АТОМНОГО ЯДРА
2003. Т. 34. ВЫП. 4

УДК 539.1.074.3, 539.172.5

NEUTRON DETECTION METHOD IN THE STUDY OF THE MUON CATALYSIS PROCESS

V. V. Filchenkov

Joint Institute for Nuclear Research, Dubna

ФИЗИКА ЭЛЕМЕНТАРНЫХ ЧАСТИЦ И АТОМНОГО ЯДРА
2003. Т. 34. ВЫП. 4

УДК 539.1.074.3, 539.172.5

NEUTRON DETECTION METHOD IN THE STUDY OF THE MUON CATALYSIS PROCESS

V. V. Filchenkov

Joint Institute for Nuclear Research, Dubna

The review is devoted to the experimental method for the muon catalysis investigation based on the detection of neutrons produced in the negative muon catalyzed fusion reaction. This method has a great advantage over others, because it allows measurements in a wide range of temperatures and densities of D/T or H/D/T mixtures, which is very important for the full knowledge of the investigated process. This paper is predominantly based on the investigations of the Dubna group which achieved a high progress in the method development concerning both the detector parameters and the new analysis means.

Обзор посвящен экспериментальному методу изучения процесса мюонного катализа (МК), основанному на регистрации нейтронов от индуцированных мюоном ядерных реакций синтеза. Этот метод обладает важными преимуществами перед остальными, так как позволяет проводить исследования МК в широком диапазоне температур и плотностей смеси изотопов водорода, что важно для всестороннего знания изучаемого процесса. Работа основана, главным образом, на результатах, полученных группой ЛЯП ОИЯИ (Дубна), достигшей наибольших успехов в развитии детекторов и методов анализа экспериментальных данных.

INTRODUCTION

The experimental discovery of the muon catalyzed fusion (MCF) process [1] and the first investigations of this phenomenon were made with the bubble chambers [2]. Extensive studies of μ-atomic and μ-molecular processes were carried out by the Dubna group with the diffusion cloud chamber [3]. It is in those experiments the phenomenon of the $dd\mu$-molecule resonance formation was first revealed. The counter technique in the MCF study was first employed in [4] and then successfully developed by L. Lederman's group [5]. The NaI detectors were used in those works to detect γ quanta from the fusion reaction $pd\mu \to {}^3\mathrm{He}\mu + \gamma + 5.4$ MeV. A unique combination of the counter technique and the track device was demonstrated by the Gatchina group in investigations of the MCF process in deuterium and D/T mixture [6]. The charged products of the MCF reactions $d + d$ and $d + t$ were detected by the ionization chamber. This method is characterized by important advantages such as high spectrometric properties and 100 % detection efficiency but has serious limitations in the gas filling parameters (density, temperature, and tritium contamination) and time resolution.

The neutron detection method consists in registration of neutrons from the fusion reactions

$$d + d \longrightarrow {}^3\mathrm{He} + n + 3.3 \text{ MeV}, \tag{1}$$

$$d + t \longrightarrow {}^4\mathrm{He} + n + 17.6 \text{ MeV}, \tag{2}$$

$$t + t \longrightarrow {}^4\mathrm{He} + n + n + 11.3 \text{ MeV}. \tag{3}$$

This method allows measurements in a wide range of the experimental conditions and also the investigation of the temperature and density dependence of the MCF parameters. That is why this method is most spread in different laboratories (Dubna, PSI, LAMPF, RIKEN–RAL).

For the first time, the neutron detection of the MCF reactions was employed by the Dubna group in the experiment with a gaseous deuterium target [7]. Few years ago, the authors used this method in the measurements of the temperature dependence of the $dd\mu$-molecule formation rate where the direct proof of the resonance character of the MCF process was obtained [8]. Later the authors achieved high progress in the method development concerning both the detector parameters and the new analysis means.

1. DETECTORS

Scintillation detectors with an organic scintillator are used in MCF experiments based on the neutron registration. This is mainly due to their large detection efficiency. In such detectors the scintillation light produced by the recoil protons is collected on the photomultiplier (PM). The amplitude spectrum reflects the proton energy distribution extending from zero to the maximum value equal to the neutron energy. The cross section for the $n{-}p$ interaction is 2.5 b for 2.5 MeV neutrons from the $d + d$ reaction and 0.7 b for 14 MeV neutrons from the $d + t$ reaction, which corresponds to the detection efficiency per the scintillator thickness unit $\simeq 10$ %/cm and $\simeq 3$ %/cm, respectively. Another important advantage of such detectors consists in the possibility of realizing the neutron-gamma separation in (liquid and crystalline) scintillators and, thus, essentially discriminating a background.

In the experiment [7], the Dubna group used a neutron detection system consisting of nine detectors, each a $\oslash 70 \times 30$ mm stylben scintillator [9]. Many-parameter analysis was employed provided the flexible use of the selection criteria. Neutron-gamma separation was made by comparison of the total charge of the detector signal and the charge of its fast component. Due to relatively small scintillator dimensions the detection efficiency was not so large and amounted to only a few per cent.

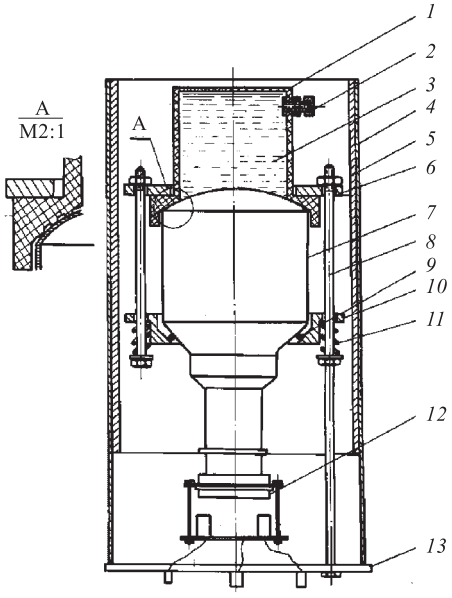

Fig. 1. Scheme of the neutron detector with an «open» cuvette: *1* — teflon cuvette; *3* — liquid scintillator; *7* — PM

In the pioneering experiment [10], where MCF reaction (2) was first detected, more effective detectors were used [11]. Neutrons were detected by four detectors with the NE-213 liquid scintillator. The scheme of the detector is shown in Fig. 1.

The novel idea underlay in the detector design. A teflon cuvette 95 mm in height and 100 mm in diameter was directly connected with the PM without any transparent materials and light guide. This original design with a highly effective reflector allows essential improvement of the spectrometric properties of the detector as compared with the «standard» detectors with a glass or metallic cuvette. So, the energy resolution was equal to $\sigma = 0.12/E_{ee}$ (MeV) %. Here E_{ee} is the so-called equivalent (on the scintillator light yield) electron energy.

Detectors used later by other groups [12–14] for the MCF study were of approximately the same size but had the worse energy resolution. The main two neutron detectors in [12] used $\oslash\, 12.7 \times 10$ cm NE-213 (volume 1.3 l). The LAMPF group [13] used the detector with Bicron BC-501 liquid scintillator with volume 1.6 l. In the RIKEN–RAL experiments [14] neutrons were detected by two NE-213 detectors of relatively small size ($v \simeq 0.5$ l).

The dominant achievement of the Dubna group was the realization of the full absorption neutron detector (FAND) [15], which surpasses essentially other detectors in the detection efficiency and has better spectrometric properties. The preliminary investigations of the properties of NE-213 and teflon as a light reflector were made [16]. Both the NE-213 scintillator optical transparency and the optical reflection coefficient of a teflon were independently measured for the first time. The improved analysis of the data [16] was done in [17]. It turned out that, contrary to the previous data obtained by other authors, NE-213 has a very high transparency. The light attenuation length was measured to be $\xi = (4.69 \pm 0.07)$ m. As to teflon, its reflection coefficient (r) was found to be $r = 0.970 \pm 0.002$ which is very high. This made possible good parameters for a detector of very large size to be obtained.

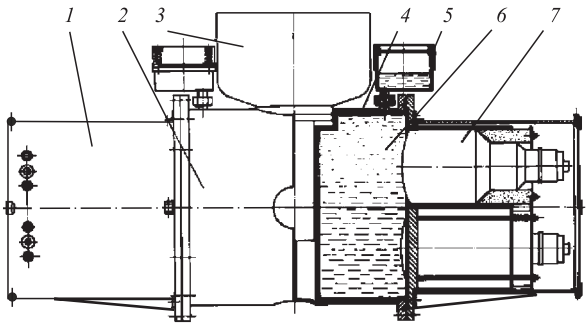

Fig. 2. Scheme of the full absorption neutron detector: *2*, *6*, and *7* are the cuvette, scintillator and PM, respectively

The spectrometer consists of two identical parts symmetrically placed around a target. The total scintillator volume of two detectors was 22 litres. The NE-213 liquid scintillator was used for registration of reaction (1) with $n-\gamma$ separation and the plastic scintillator for investigation of MCF reaction (2). The scheme of the FAND is shown in Fig. 2.

The main ideas of [11] were used for the design of the FAND. As in detectors [11], PM's contact directly with the scintillator, and teflon is used as a reflector. Four PM (XP 2041) view the 11-litre cuvette filled with NE-213. The cuvette was made of stainless steel, its internal surface was laid with teflon. Both detectors are placed in the immediate vicinity of the target which provides a large solid angle (65 %) of the system. This allowed a decrease in the external background. The intrinsic detection efficiency was $\simeq (50-70)\,\%$ for neutrons from reaction (1) and $40-50\,\%$ (depending on the energy threshold) for neutrons from reaction (2).

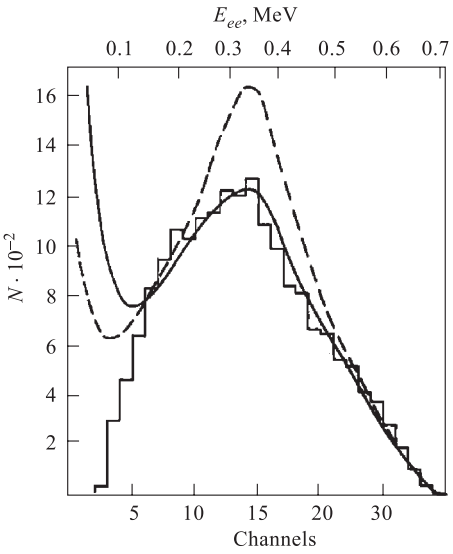

Fig. 3. Charge distribution measured in [18] with a high-density deuterium target and the FAND (histogram). The solid line is the Monte-Carlo calculations [19]; the dashed line corresponds to a «bare» detector

Contrary to the usual «grey» detector where amplitude distribution reflects the *single interaction* recoil proton spectrum, the full absorption («black») detector provides the enhancement of the high-amplitude part of the distribution resulting from the almost full loss of the neutron energy in *multiple scatterings*. This allows a decrease of the detection efficiency loss and the appropriate uncertainty connected with the threshold influence.

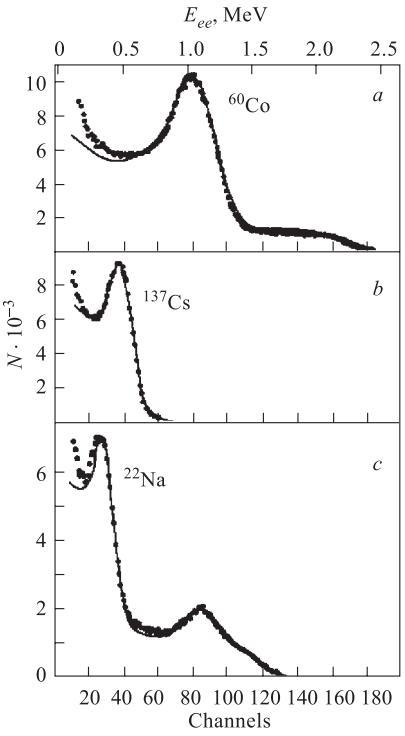

Fig. 4. Compton electron spectra measured with ^{60}Co (*a*), ^{137}Cs (*b*), and ^{22}Na (*c*) γ sources. Lines correspond to the Monte-Carlo calculations with the optimum value of the energy resolution [20]

The charge distribution of the FAND for neutrons from reactions (1) is shown in Fig. 3. The specific shape of the FAND charge spectrum is most clearly manifested for a «bare» detector (dashed line). The real spectrum (histogram) measured with a high-density deuterium target is distorted due to specific character of $n-d$ interaction. Nevertheless, it differs radically from the one measured with «grey» detectors.

Close packing of the PM's, their direct contact with the scintillator, and the use of teflon as the light reflection material provided high spectrometric properties of the FAND. The analysis of the light collection process in the FAND was performed in [17]. It turned out that the total collection efficiency is $\simeq 70\,\%$ and the dominant part ($> 95\,\%$) of light is collected on PM's during 25 ns. (*It is remarkable that the light collection process in time can be described with the same mathematics which is used for the time spectrum of the first detected neutrons in the MCF process. For this, one should identify light attenuation with muon decay, light loss in reflection with muon sticking, and PM's geometrical efficiency (relative surface of their cathodes) with the neutron detection efficiency [17].*)

The Compton electron spectra obtained with the γ sources of ^{137}Cs (0.667 MeV), ^{60}Co (1.17 and 1.33 MeV) and ^{22}Na (0.51 and 1.28 MeV) are shown in Fig. 4 [20]. The high detection efficiency allowed confident simultaneous registration of two γ quanta with the total energy of 2.5 MeV from the ^{60}Co and of 1.69 MeV from the ^{22}Na sources. The parameters of the FAND

were found from the analysis of the spectra shown in Fig. 4 with the use of the Monte-Carlo simulated distributions [20]. The energy resolution was found to be $\sigma = 5.6\sqrt{1 + 10/E_{ee}}\,\%$ (FWHM).

Special investigations were carried out to study the time properties of the detector. The shape of the detector signal is determined by two processes — scintillation light irradiation and light collection on PM. Both processes were involved in the analysis which was performed in [17]. The results of the corresponding calculations are shown in Fig. 5 for detectors of different size in comparison with the measurements. As one can see, they describe the real signals well.

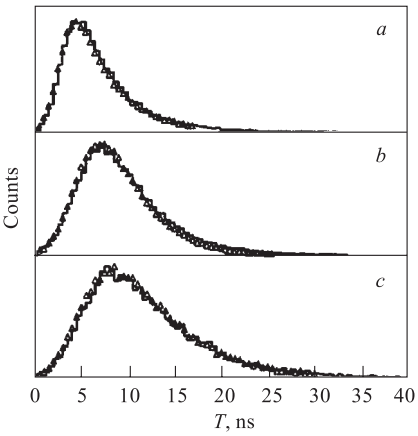

Fig. 5. The detector pulse shapes for the $2 \times 2 \times 0.5$ cm plastic scintillator and XP-2020 PM (*a*); for $\varnothing$ 10×9.5 cm NE-213 scintillator with XP-2040 PM (*b*); and for $\varnothing$ 31×16 cm neutron spectrometer [15] (*c*). The measurement results are shown by triangles connected with lines, and the Monte-Carlo calculations are presented as histograms

The FAND time resolution was determined in [21] with a γ source by measuring coincidence between signals from the FAND and a small-size detector. It turns out that the FWHM of the time resolution curve is only 3.1 ns. Of course, the spread in the neutron time of flight from the target to the detector deteriorates the time resolution. As follows from the Monte-Carlo calculations for 2.5 MeV neutrons, the time resolution function is well described by the Gaussian with the width of 5.6 ns. Finally, if one takes into account the time registration system with a flash ADC, the full width of the time resolution curve becomes equal to 13 ns.

Good timing properties gave us the possibility of precisely measuring the parameters of the fast (tens of ns) component of the time spectra while investigating the MCF $d + d$ reaction in deuterium [18, 22].

The principal problem of the neutron method is knowing the absolute detection efficiency ϵ_n. It is not a trivial task to determine ϵ_n for organic scintillation counters because it is influenced by factors like the geometry of the surrounding material, generation of light by various reaction products and because many energy-dependent cross sections are involved. Because of lack of neutron calibration sources with the well-known intensity and sufficiently large energy, the efficiency had to be calculated. The Monte-Carlo technique was used for this purpose.

Calculations of ϵ_n for neutrons detected by the FAND in the Dubna experiments are described in [19,25]. The CERN package GEANT was used in [25] for the simulation calculations. Because it lacks the appropriate low and fast neutron interaction cross sections, GEANT was linked with the MICAP [26] package. MICAP uses experimental neutron cross sections from the ENDF/B-VI data base from 20 MeV down to thermal energies (10^{-5} eV). This includes: partial cross sections, angular distributions, energy distributions of reaction products and deexitation photons. The preprocessed ENDF/B-VI data represent the experimental data within 2 %.

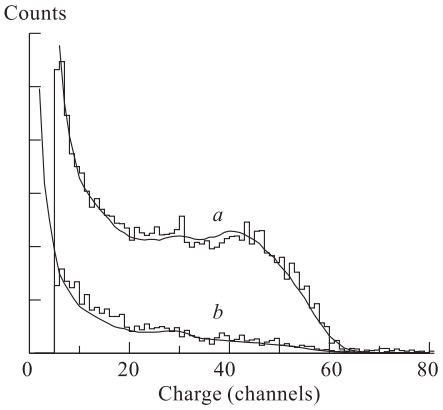

Fig. 6. Charge distribution for 14 MeV neutrons measured in [27] with the FAND (histograms). Distributions are plotted for single (*a*) and coincident (*b*) events. Lines are the Monte-Carlo calculations [25]

After the calculation of the energy deposited inside the scintillator, the electronic output signal was obtained by first converting the energy into scintillation light considering the particle type, and then converting the total light output into an electric signal by applying the detector response function [20]. This function takes account of factors such as nonuniform light collection depending on the position of light generation inside the scintillator and photon statistics. The results of calculations [25] for 14 MeV neutrons from reaction (2) are presented in Fig. 6 together with the measured spectra.

One neutron detected in a scintillator may generate a response from one detector or, due to scattering or to generated gamma rays, from both detectors. This leads to a single and coincident rate. The corresponding spectra are shown in Fig. 6 together with the measured ones. As is seen, there is a good agreement between the measurements and calculations for both cases (single and coincident). The intensity and amplitude calibration of the calculated single spectrum was normalized to single data. The normalization thus obtained is then applied to the calculated coincident spectrum, which then neatly coincides with the corresponding data. This means that the single-to-coincident ratio is well predicted, which is considered to be a sensitive validation check for the calculations. The estimated relative uncertainty in ϵ_n is not worse than 5–7 %.

The neutron detection system with FAND was successfully used under study of the MCF process in solid, liquid and gaseous deuterium [18, 22, 23] and for investigation of the muon transfer from deuterium to helium [24]. The most

effective realization of the neutron method with high efficiency detectors was demonstrated in experiments on the systematic study of the MCF $d + t$ fusion process (see, for example, [27–29]).

2. INVESTIGATION OF THE MCF $d + t$ PROCESS

2.1. Experimental Method. The principal quality of the Dubna MCF experiments is that we use high-density (solid, liquid or gas) targets filled with D/T or H/D/T mixture. This provides very high multiplicity (~ 100) of neutrons produced by a single muon during its life time (2 μs). High intensity of detected events results in definite difficulties connected with pile-up. This effect seems to be more essential for a high-efficiency detection system used by us. However, we were able not only to solve the pile-up problem but also to receive a profit from the high neutron multiplicity. Special methods were developed for this.

The principal features of our experimental method are the following:

1. A high efficiency neutron detection system is used in the close to 4π geometry.

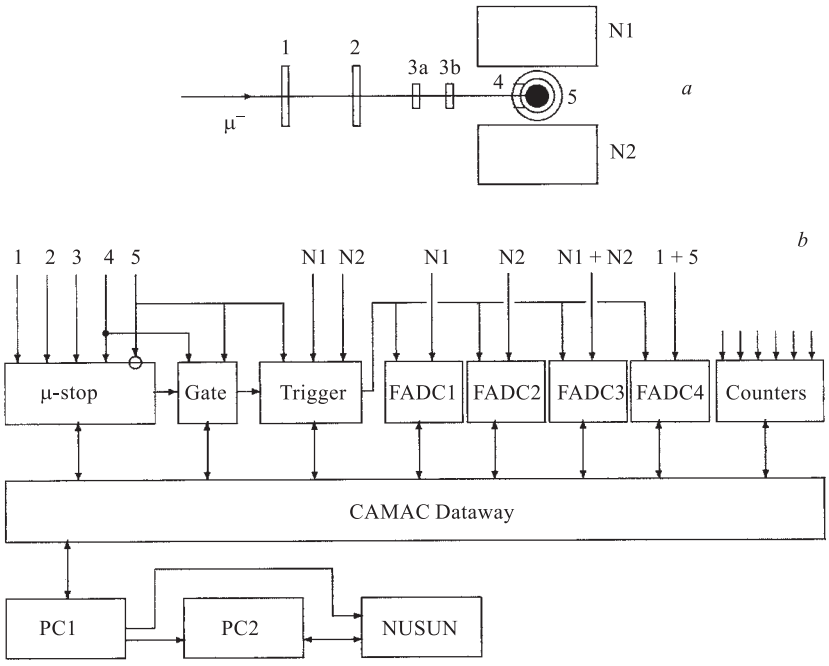

Fig. 7. Scheme of the experiment: N1 and N2 are the FAND; 1–3 are the detectors for incoming muons; 4 and 5 are the wire proportional counters

2. For muon and electron registration we use specially designed wire proportional counters with very low sensitivity to neutrons.

3. To eliminate the distortions caused by pile-up, the charge time distributions for the neutron detector signals are measured, contrary to the usually registered time distributions of the number of events. Flash ADC are used for this aim.

4. Novel methods for the data analysis are used which are most effective for the case of high neutron multiplicity.

The scheme of the experiment is shown in Fig. 7.

The installation was mounted on the muon beam of the JINR Phasotron. The main parts of the experimental set-up are a compact cryogenic target, a wire electron counter [30] and a full absorption neutron spectrometer [15], consisting of two identical detectors (N1 and N2).

Pulses from the PM of the neutron spectrometer are registered by flash ADC (8 bit $\times$ 2048 samples, 100 Mc/s) producing a time distribution of the N1, N2 signal amplitude for each single muon. To provide correct time measurements, the signals of the detector for incoming muons and the electron counter are also analyzed by flash ADC. The example of «oscillograms» observed on flash ADC is shown in Fig. 8.

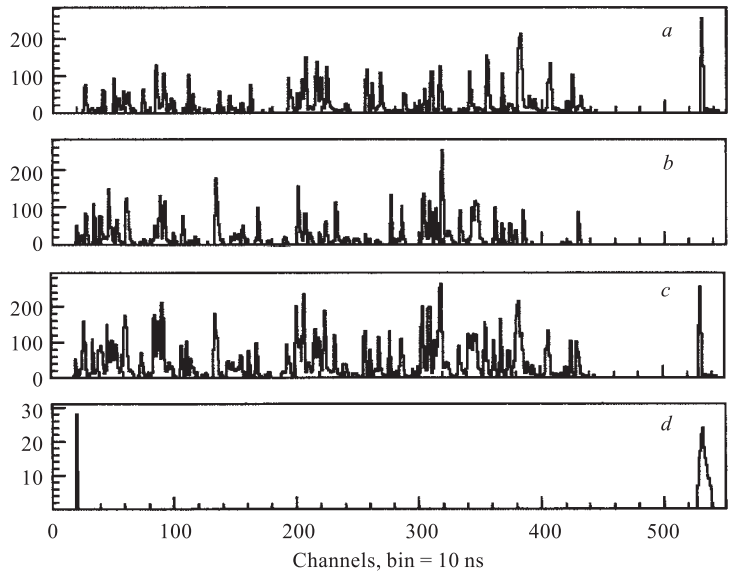

Fig. 8. Flash ADC signals for a single muon. The signals are shown for N1 (*a*), N2 (*b*) N1 and N2 together (*c*) and for the muon and electron detectors (*d*)

The trigger equirements included the presence of the signals of muon stop (1, 2, 3a, 3b, 4, 5) and electron (5 or $5, \mathrm{N1} + \mathrm{N2}$) during the time gate 20 μs long starting by the incoming muon signal $(1, 2)$. Insertion of the electron signal in the trigger makes it possible to radically suppress a background connected with the muon stops in the target walls, where muon undergoes predominately (90 %) nuclear capture without electron escape. Additional suppression of this background is achieved at the condition when only delayed electrons (later than 0.2 μs after the gate start) are permitted.

Another important advantage of this is that the direct normalization on the electron number becomes possible without a necessity to determine the number of muon stops in hydrogen. This method was firstly employed by us in the first experiment on the MCF $d+t$ reaction [10] and allows the successful performance of this fundamental work.

2.2. Analysis Methods. The most popular and practically the only method used by most groups involved in the study of the MCF $d + t$ process is the so-called standard method where the yield and time distribution of all detected neutrons from reaction (2) are registered and analyzed. This distribution has the well-known one-exponent form

$$dN_n/dt = \epsilon_n \Lambda_c \exp\left[-(\lambda_0 + W\Lambda_c)t\right]. \tag{4}$$

Here $\Lambda_c = \lambda_c \phi$; ϕ is the hydrogen density relative to the value $4.25 \cdot 10^{22}$ nuclei/cm^3; $\lambda_0 = 0.455 \cdot 10^6$ s^{-1} is the free muon disappearance rate; ϵ_n is the neutron detection efficiency; W is the effective muon loss in the $d+t$ cycle which includes the muon sticking to helium in the $d+t$, $d+d$ and $t+t$ reactions. The number of electrons from μ decay N_e is used for normalization

$$N_n/N_e = \epsilon_n \Lambda_c/[\lambda_0 + W\lambda_c]. \tag{5}$$

The slope of exponent (4) and the normalized neutron yield are the measured parameters. The values of Λ_c and W are extracted from (4) and (5).

In the Dubna experiments, we also used the standard method. To obtain the spectrum (4) we created the time distribution of the neutron detector charge $Q(t)$. For this we summed the amplitude spectra for each neutron detector shown in Fig. 8. Then the spectrum $Q(t)$ was transformed to the time distribution of the number of events $N_n(t)$ using the *unit charge* [31]. The latter was measured in special conditions providing the low neutron multiplicity, where each charge pulse corresponds to one neutron. Charge distributions obtained in such exposures were compared with the calculated ones to obtain the experimental value of ϵ_n as a function of the threshold.

The principal disadvantage of the standard method is that the main MCF parameters — cycling rate and effective muon losses — are not obtained directly, only their product is measured directly. In our measurements we employed two

novel independent methods suggested and developed in Dubna [32, 33]. These analysis methods make it possible to directly measure the values of λ_c and W. A suggestion of [32] was to measure the distribution $N_{ne}(t)$ which is a function of the interval $t = t_e - t_n$ between the last detected neutron of the series and the μ-decay electron. This distribution has the form of a sum of two exponents with significantly different slopes [32, 33]

$$dN_{ne}/dt = (\lambda_0/\lambda_n)[W\Lambda_c \exp(-\lambda_0 t) + \epsilon_n\Lambda_c(1-W) \exp(-(\lambda_0+\lambda_n)t)], \quad (6)$$

where λ_n is expressed as

$$\lambda_n = (\epsilon_n + W - \epsilon_n W)\Lambda_c. \quad (7)$$

The first («slow») exponent corresponds to the events with muon sticking and the second («fast») one to the events without sticking. The cycling rate is determined from the fast component slope, and muon loss is obtained from the ratio of the amplitudes of slow and fast exponents: $A_s/A_f = W/\epsilon_n(1-W)$. The examples of such distributions obtained in a liquid D/T mixture are presented in Fig. 9. As is seen from the figures, the events with and without sticking are clearly separated. Different slopes of the fast components of the spectra reflect the different values of cycling rate realized for the tritium concentrations $C_T = 35.8\,\%$ and $C_T = 88.5\,\%$. The advantage of the method is that charge calibration is not necessary in this case.

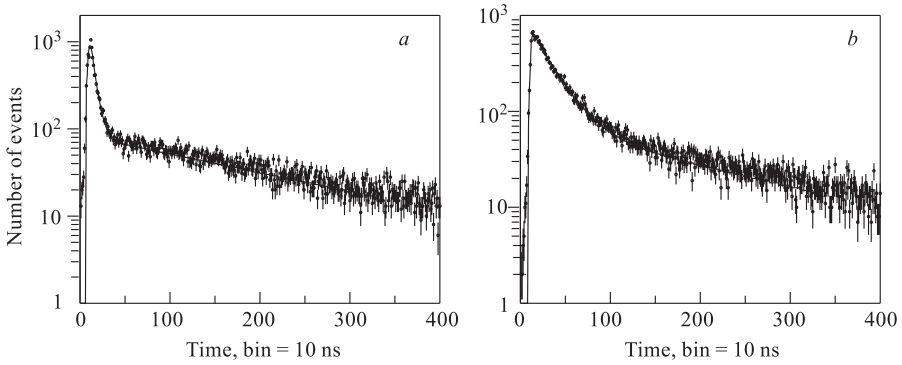

Fig. 9. Electron-last neutron timing spectra measured with a liquid D/T mixture. Spectrum *a* corresponds to the exposure with $C_T = 35.8\,\%$ and variant *b* was selected for $C_T = 88.5\,\%$. Lines are the fit with expression (6) and the optimum parameters $\epsilon_n\Lambda_c$ and W/ϵ_n

Another idea [33] was to measure the neutron multiplicity (number of detected neutrons, k, per muon) distribution in some definite interval T. If one selects the events for which the muon does not decay in this interval, then this distribution would be a sum of two terms. One of them, the Gaussian (Poisson) with the mean $m = \epsilon_n \Lambda_c T$, corresponds to the events without sticking, and the other, depending on W and falling with k, is the distribution of events with muon sticking:

$$N(k) = N_1[f(k) + (1 - W/\epsilon_n)^m g(k; m)], \tag{8}$$

where N_1 is the total number of the first detected neutrons in the interval T; $g(k; m)$ is a Gaussian and $f(k)$ is described as

$$f(k) = y_{k-1} - y_k = y_1[1 - y_1(1 - W)][y_1(1 - W)]^{k-1},$$

where $y_1 = \epsilon_n \Lambda_c / \lambda_n = (1 - W/\epsilon_n - W)^{-1}$ is the relative yield of the first detected neutrons. So, as in the previous method, there is a separation of the events with and without sticking.

Examples of the neutron multiplicity distributions (charge normalized) are given in Fig. 10. Such distributions for each exposure were fitted with formula (8). The quantities W/ϵ_n and the Gaussian (Poisson) mean $m = \epsilon_n \Lambda_c T$ were variable parameters. Other parameters were the total number of events and the dispersion of the Gaussian. The optimal fit is shown by the curve.

The original expression (8) is «phenomenological» and approximate. Surprisingly, it describes rather well the multiplicity distributions in a wide interval of m. So, for $m = 8{-}40$ fit of the appropriate Monte-Carlo (M-C) spectra with

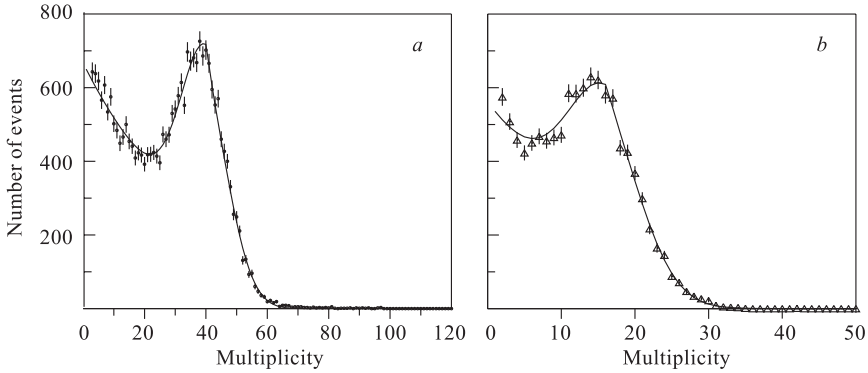

Fig. 10. Neutron multiplicity distributions measured with a liquid D/T mixture. Spectrum *a* corresponds to the exposure with $C_T = 35.8\,\%$ and was plotted for both ND and time interval $T = 1$ μs. Variant *b* was selected for $C_T = 88.5\,\%$, both for ND and $T = 2$ μs. Curves are the optimum fits

formula (8) gives the results coinciding with the predicted ones within $3{-}4\,\%$. Of course, the accurate analysis needs a rigorous expression for the multiplicity distribution accurate over the entire range of m.

The rigorous expression was obtained in [34]. It has the form

$$f(k) = \frac{[\epsilon(1-W)]^k}{(\epsilon+W-\epsilon W)^k} P(k) + \frac{[\epsilon(1-W)]^{k-1} W}{(\epsilon+W-\epsilon W)^k} F(k), \tag{9}$$

where $P(k)$ is the Poisson distribution with the mean $m = \lambda_n T$

$$P(m) = \frac{(\lambda_n T)^k}{k!} \mathrm{e}^{-\lambda_n T},$$

$$F(k) = 1 - \mathrm{e}^{-\lambda_n T} \sum_{i=0}^{k-1} \frac{(\lambda_n T)^i}{i!},$$

and λ_n is given by formula (7). Formula (9) corresponds to the «event mode», where the number of detected neutrons was considered. Really the distributions of the neutron detector $charge$ are measured in experiments and were divided by the $unit\ charge$ to obtain a multiplicity distribution. The real response function of the detector results in diffusion of the measured spectra as compared with the ones obtained in the «event mode». It turned out that in good approximation (with accuracy of 2–3 % in cycling rate), the real distribution might be obtained as convolution of formula (9) with the Gaussian function. The Gaussian width is varied to obtain the best agreement between the experiment and calculations.

In experiments with a high density D/T and H/D/T mixture at temperatures to 800 K, the targets with rather thick walls are used. This leads to noticeable (50 %) losses of electrons reaching the electron counter and thus to a decrease in statistics. Another essential loss of electrons arises during the procedure of their confident identification. The multiplicity method allows an increase in the measurements efficiency. For this, one should exclude the requirement of the electron signal in the trigger and select only those neutron series whose duration is larger than the chosen interval T. Of course, only λ_c can be determined in this case since events without muon sticking to helium are accepted. An example of the multiplicity distribution selected with this criterion is shown in Fig. 11.

The comparison of all methods used by us in the analysis is given in the Table.

The statistical power is practically the same for all the methods. Indeed, in the standard method the main factor for the statistical accuracy is the limited number of electrons, the number of neutrons is much higher under real experimental conditions. In two other methods, the full statistics is the number of the first or last neutrons which are also approximately equal to the electron number.

In our investigations we use all three mentioned methods. It allows us to realize the confident data analysis with minimum systematic uncertainties. Of course, the full analysis is rather complicated and includes many tests with different selection rules for events to be accepted.

As follows from our experience, the main problem is connected with the electron identification. In the conditions when one muon can cause ~ 100 fusion neutrons it is possible to take a neutron for an electron, which yields in distortion of results. Even in our case, where a wire counter for electron detection is used, this possibility can be noticeable. To exclude the false electrons, the following criteria are used under the event selection:

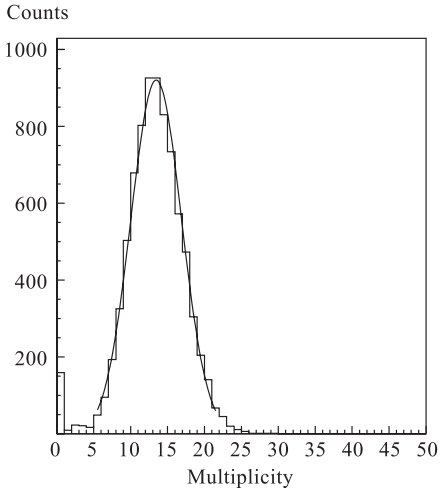

Fig. 11. Experimental multiplicity distribution accumulated for the time interval $T = 1$ μs and selected under the criterion $t_n^{\rm last} > T$. The line is the Gaussian with the optimum parameters found in the fit

— require coincidence between the signals of electron and neutron detectors;

— put the threshold for the energy loss in neutron detector large enough ($\simeq 10$ MeV) to exclude the neutron in electron identification.

The results of our consideration show that ambiguities in the main MCF parameters caused by the false electron, decrease to 3–4 % if these requirements are obeyed.

Comparison of different methods used in the MCF study

Method	λ_c, W determination	Charge calibration	Electron detection
Standard	Indirect	Necessary	Required
$t_e - t_n$	Direct	Not required	Required
Multiplicity	Direct	Required	Not necessary

Note that determination of the cycling rate by the multiplicity method is free from these ambiguities because the position of the peak in the multiplicity distribution does not depend on selection criteria. So we have an excellent test for the results obtained by other methods.

Another problem is how the neutron detection efficiency depends on the neutron multiplicity (cycling rate). The main idea of using the flash ADC is that the total charge per number of neutrons is conserved even when the ND signals mostly overlap. However, it is true only for the zero charge threshold. Really, the cluster charge should be limited to reduce the low-energy background.

At a high neutron multiplicity, clusters of small charge can overlap with one or more others and, hence, can be accepted (noneffective threshold). Obviously, this results in an increase of the detection efficiency as compared with the low neutron multiplicity. The real increase depends on several factors, such as the shape of the ND signal, the form of the response function, the magnitude of the threshold and the measured cycling rate. Since one would expect an essential correction to the value of ϵ_n, the problem required special consideration.

This was made in [35] where the fusion neutron registration was Monte-Carlo simulated for a wide cycling rate. All three analysis methods were considered. It turned out that in the standard and multiplicity methods corresponding corrections to the efficiency are not so large. So, even for the maximum possible measured cycling rate $\epsilon_n \Lambda_c = 40\ \mu\text{s}^{-1}$ they are only 12 %. It is due to the fact that the dominate yield to the total charge gives the large amplitudes which are much more than the threshold. Contrary to the *«collective» events* methods (standard and multiplicity), the $t_e - t_n$ method is based on consideration of *individual events*. That is why the corrections to efficiency are relatively large in this case and can amount to 25 %.

As the analysis procedure is correct, the results obtained by the different methods should be identical. As follows from [27], it is really true within an accuracy of 5 %. It follows from our consideration that the main sources of possible systematic errors are connected with ambiguities in the ϵ_n calculations and the charge calibration. In total, they do not exceed 10 %.

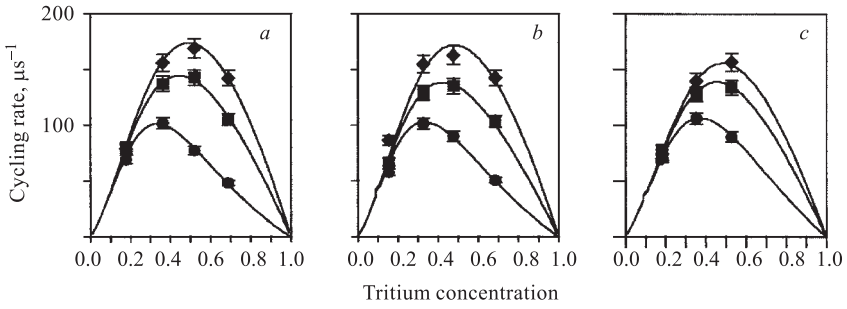

Fig. 12. Measured values of λ_c as functions of temperature for different densities: *a*) $\phi =$ 0.3 LHD; *b*) $\phi = 0.4$ LHD; *c*) $\phi = 0.5$ LHD. Circles — $T = 300$ K; squares — $T = 550$ K; rhombuses — $T = 800$ K. The data are taken from [37]

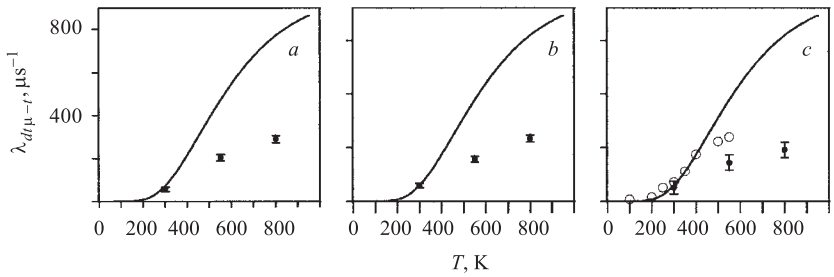

Fig. 13. The values of $\lambda_{dt\mu-t}$ (points) as functions of temperature obtained from the cycling rate analysis compared with theory (lines) [38] and other measurements [13] (empty points). *a*) $\phi = 0.3$ LHD; *b*) $\phi = 0.4$ LHD; *c*) $\phi = 0.5$ LHD

Some of the main results are presented in Figs. 12–14. The values of the $dt\mu$-molecule formation on molecules D_2 ($\lambda_{dt\mu-d}$) and DT ($\lambda_{dt\mu-t}$) were extracted from the analysis of the cycling rate as a function of the tritium concentration in the D/T mixture. These dependences are shown in Fig. 12.

It follows from our analysis that, in accordance with the theory, the value of $\lambda_{dt\mu-t}$ sharply depends on temperature. The corresponding dependences are given in Fig. 13. Comparison of our data with the calculations [38] allows the conclusion that the theoretical values of the resonant $dt\mu$-molecule formation rate are larger than the experimental ones. This coincides with the opinion of the authors of the experiment [39] conducted at PSI with the D/T mixture of density $\varphi = 0.05$. Note that measurements [39] were made at the temperature $T = 30$ K, and the effect of $dt\mu$ formation on DT could be observed only as an epithermal effect. Contrary to the case of $\lambda_{dt\mu-t}$, the value of $\lambda_{dt\mu-d}$ depends only slightly on temperature. On the other hand, this value depends noticeable on density, as is evident from Fig. 14. This indicates a significant role of the triple collisions in the $dt\mu$-molecule formation process.

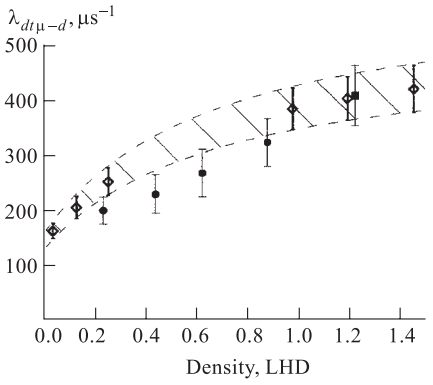

Fig. 14. Density dependence of the $dt\mu$-molecule formation rate. Squares are the Dubna measurements [37] ($T = 22$ K (liquid)); circles — $T = 74.5$ K (gas); rhombuses are the results [39] (PSI data); the dashed region corresponds to the parameterization made in [39]

CONCLUSION

The neutron detection system based on the FAND is successfully used in the MCF study at the JINR Phasotron. A high efficiency of the system allows a high statistics to be taken even for relatively low muon intensity provided by the accelerator. Moreover, the new special methods have been developed which are the most effective just for the high registered neutron multiplicity. In future we plan to continue the experimental investigation of the MCF process using this system.

In particular, we intend to study the MCF reaction (3) in liquid tritium. Our system consisting of two oppositely placed high-efficiency detectors gives an excellent possibility of determining the MCF parameters, such as the $tt\mu$-molecule formation rate $\lambda_{tt\mu}$ and the coefficient of muon sticking to helium ω_{tt}, and studying two-particle correlations in the final state of the fusion reaction. The reasons for this are the following.

1. The high neutron detection efficiency ϵ_n allows the high statistics of the second detected neutrons ($\sim \epsilon_n^2$) and thus precise determination of ω_{tt} from the relation

$$1 - \omega_{tt} = \eta_2/\eta_1^2,$$

where η_1 and η_2 are the yields of the first and second detected events, respectively [36].

2. The charge distribution shape of the effective neutron detector is very sensitive to the yield of the $\alpha{-}n$ or $n{-}n$ interactions.

3. Two-particle correlations can also be observed by comparison of the single detector events and the coincidences between two detectors. Both for the $\alpha{-}n$ and $n{-}n$ correlations the single events should dominate while the essential yield of coincidences should be in the absence of correlations (pure phase space).

Acknowledgements. The author would like to thank T. N. Mamedov and V. G. Zinov for valuable remarks.

REFERENCES

1. *Alvarez L. W., Bradner H., Crawford F. S.* // Phys. Rev. 1957. V. 105. P. 1127.
2. *Fetkovich J. G. et al.* // Phys. Rev. Lett. 1960. V. 4. P. 570;
   Doede J. // Phys. Rev. 1963. V. 132. P. 1782.
3. *Dzhelepov V. P. et al.* // JETP. 1964. V. 46. P. 2042.
4. *Ashmore A. et al.* // Proc. Phys. Soc. 1958. V. 71. P. 161.
5. *Bleser E. J. et al.* // Phys. Rev. 1963. V. 132. P. 2679.
6. *Balin D. V. et al.* // JETP. 1984. V. 40. P. 318.
7. *Bystritsky V. M. et al.* // JETP. 1974. V. 66. P. 61.

8. *Bystritsky V. M. et al.* // Proc. of the 7th Intern. Conf. on High Energy Physics and Nuclear Structure, Zurich, Aug. 28–Sept. 3, 1977 / Ed. M. Locher. Basel, 1977.
9. *Bystritsky V. M. et al.* // PTE. 1972. V. 1. P. 65.
10. *Bystritsky V. M. et al.* // Phys. Lett. B. 1980. V. 94; JETP Lett. 1981. V. 53. P. 877.
11. *Zinov V. G. et al.* // PTE. 1982. V. 1. P. 26.
12. *Beunlich W. H. et al.* // Muon Cat. Fusion. 1987. V. 1. P. 67;
Ackerbauer P. et al. // Nucl. Phys. A. 1999. V. 652. P. 311.
13. *Jones S. E. et al.* // Muon Cat. Fusion. 1987. V. 1. P. 53;
Jones S. E. et al. // Phys. Rev. Lett. 1986. V. 56. P. 588.
14. *Matsuzaki T. et al.* // Hyp. Int. 1999. V. 118. P. 229.
15. *Dzhelepov V. P. et al.* // Nucl. Instr. Meth. A. 1988. V. 269. P. 634.
16. *Zinov V. G., Konin A. D., Filchenkov V. V.* // Nucl. Instr. Meth. A. 1985. V. 245. P. 490.
17. *Baranov V. A. et al.* // Nucl. Instr. Meth. A. 1996. V. 374. P. 335.
18. *Dzhelepov V. P. et al.* // JETP. 1992. V. 101. P. 1105.
19. *Filchenkov V. V., Marczis L.* Registration Efficiency of a Full Absorption Neutron Spectrometer. JINR Commun. E13-88-566. Dubna, 1988.
20. *Filchenkov V. V., Konin A. D., Rudenko A. I.* // Nucl. Instr. Meth. A. 1990. V. 294. P. 504.
21. *Zinov V. G. et al.* JINR Commun. 13-911-82. Dubna, 1991; PTE. 1992. V. 4. P. 59.
22. *Demin D. L. et al.* // Hyp. Int. 1996. V. 101/102. P. 591.
23. *Demin D. L. et al.* JINR Preprint E15-2002-157. Dubna, 2002.
24. *Bystritsky V. M. et al.* // JETP. 1990. V. 98. P. 1514.
25. *Bom V. R., Filchenkov V. V.* // Hyp. Int. 1999. V. 119. P. 365.
26. *Zeinitz C.* ftp from: uazhep.physics.arizona.edu
27. *Averin Yu. P. et al.* // Hyp. Int. 1999. V. 118. P. 111.
28. *Averin Yu. P. et al.* // Ibid. P. 121.
29. *Bom V. R. et al.* // Hyp. Int. 1999. V. 118. P. 103.
30. *Konin A. D.* JINR Preprint P13-82-634. Dubna, 1982.
31. *Filchenkov V. V., Drebushko A. E., Rudenko A. I.* // Nucl. Instr. Meth. A. 1997. V. 395. P. 237.
32. *Zinov V. G.* // Muon Cat. Fusion. 1992. V. 7. P. 419.
33. *Filchenkov V. V.* // Ibid. P. 409.
34. *Filchenkov V. V., Sadetsky S. M.* // Nucl. Instr. Meth. A. 2002. V. 480. P. 771.
35. *Filchenkov V. V.* JINR Commun. E15-2000-224. Dubna, 2000.
36. *Zinov V. G., Somov L. N., Filchenkov V. V.* // Nucl. Instr. Meth. 1984. V. 228. P. 174.
37. *Bom V. R. et al.* // Proc. of the Intern. RIKEN Conf. μCF-01 «Muon Catalyzed Fusion and Related Exotic Atoms», Shimoda, Japan, April 22–26, 2001. To be published in «Hyp. Int.»
38. *Faifman M. P. et al.* // Hyp. Int. 1996. V. 101/102. P. 179.
39. *Ackerbauer P. et al.* // Nucl. Phys. A. 1999. V. 652. P. 311.